Original Article | Breast Imaging

eISSN 2005-8330
https://doi.org/10.3348/kjr.2022.0974
Korean J Radiol 2023;24(7):626-639

Check for updates

Korean Journal of Radiology
KJR

Prediction of Tumor Progression During Neoadjuvant Chemotherapy and Survival Outcome in Patients With Triple-Negative Breast Cancer

Heera Yoen[1], Soo-Yeon Kim[1,2,3], Dae-Won Lee[4], Han-Byoel Lee[5], Nariya Cho[1,2,3]

[1]Department of Radiology, Seoul National University Hospital, Seoul, Korea
[2]Department of Radiology, Seoul National University College of Medicine, Seoul, Korea
[3]Institute of Radiation Medicine, Seoul National University Medical Research Center, Seoul, Korea
[4]Department of Internal Medicine, Seoul National University Hospital, Seoul National University College of Medicine, Seoul, Korea
[5]Department of Surgery, Seoul National University Hospital, Seoul National University College of Medicine, Seoul, Korea

Objective: To investigate the association of clinical, pathologic, and magnetic resonance imaging (MRI) variables with progressive disease (PD) during neoadjuvant chemotherapy (NAC) and distant metastasis-free survival (DMFS) in patients with triple-negative breast cancer (TNBC).

Materials and Methods: This single-center retrospective study included 252 women with TNBC who underwent NAC between 2010 and 2019. Clinical, pathologic, and treatment data were collected. Two radiologists analyzed the pre-NAC MRI. After random allocation to the development and validation sets in a 2:1 ratio, we developed models to predict PD and DMFS using logistic regression and Cox proportional hazard regression, respectively, and validated them.

Results: Among the 252 patients (age, 48.3 ± 10.7 years; 168 in the development set; 84 in the validation set), PD was occurred in 17 patients and 9 patients in the development and validation sets, respectively. In the clinical-pathologic-MRI model, the metaplastic histology (odds ratio [OR], 8.0; P = 0.032), Ki-67 index (OR, 1.02; P = 0.044), and subcutaneous edema (OR, 30.6; P = 0.004) were independently associated with PD in the development set. The clinical-pathologic-MRI model showed a higher area under the receiver-operating characteristic curve (AUC) than the clinical-pathologic model (AUC: 0.69 vs. 0.54; P = 0.017) for predicting PD in the validation set. Distant metastases occurred in 49 patients and 18 patients in the development and validation sets, respectively. Residual disease in both the breast and lymph nodes (hazard ratio [HR], 6.0; P = 0.005) and the presence of lymphovascular invasion (HR, 3.3; P < 0.001) were independently associated with DMFS. The model consisting of these pathologic variables showed a Harrell's C-index of 0.86 in the validation set.

Conclusion: The clinical-pathologic-MRI model, which considered subcutaneous edema observed using MRI, performed better than the clinical-pathologic model for predicting PD. However, MRI did not independently contribute to the prediction of DMFS.

Keywords: Triple-negative breast cancer; Magnetic resonance image; Treatment response; Progressive disease; Prognosis

INTRODUCTION

Triple-negative breast cancer (TNBC), which is characterized by the absence of estrogen receptors, progesterone receptors, and human epidermal growth factor receptor 2, accounts for 10% to 20% of breast cancer cases [1]. Because of the lack of molecular targets for endocrine therapy and human epidermal growth factor receptor 2 targeting agents, its treatment is mainly dependent on conventional cytotoxic chemotherapy and associated

Received: December 7, 2022 **Revised:** March 31, 2023 **Accepted:** May 1, 2023
Corresponding author: Soo-Yeon Kim, MD, PhD, Department of Radiology, Seoul National University Hospital, 101 Daehak-ro, Jongno-gu, Seoul 03080, Korea.
• E-mail: sooyeonkim41@gmail.com
This is an Open Access article distributed under the terms of the Creative Commons Attribution Non-Commercial License (https://creativecommons.org/licenses/by-nc/4.0) which permits unrestricted non-commercial use, distribution, and reproduction in any medium, provided the original work is properly cited.

Copyright © 2023 The Korean Society of Radiology

Korean Journal of Radiology
KJR

with poor survival outcomes compared to other types of breast cancer [2]. Therefore, the consideration of optimal chemotherapy and prediction of the response are critical for managing TNBC.

Progressive disease (PD) during neoadjuvant chemotherapy (NAC) for breast cancer is defined as an increase in the tumor size or development of new tumor lesions in the breast, lymph nodes, or distant organs [3]. Breast-conserving surgery for tumors with PD may be impossible, and skin grafting may be required [3]. Moreover, nodal involvement leads to extensive axillary lymph node dissection, and distant metastases may preclude curative surgical resection [4]. Despite its clinical significance, PD has not been sufficiently studied, probably because of its rarity. According to the largest study by Caudle et al. [5], the rate of PD was 3% (59/1928) among all breast cancer cases, including all subtypes, and the clinical and pathologic factors associated with PD were advanced T stage, African-American race, and negative estrogen receptor status. However, many of these factors are associated with not only PD but also pathologic complete response (pCR) [5-9]. Thus, it is necessary to identify the predictors that are independently associated with PD.

Although extensive research has been conducted to identify the imaging findings associated with pCR [10-16], to the best of our knowledge, no study has evaluated the imaging findings associated with PD. Considering the wide use of breast magnetic resonance imaging (MRI) to evaluate the response to NAC, if we can associate specific pre-NAC MRI findings with PD, then we will be able to identify patients at high risk for PD in advance and provide safer and more efficient management. More recently, in addition to conventional MRI findings, peritumoral edema on MRI has been considered an important factor for the prediction of the prognosis and aggressiveness of tumors [17].

Breast cancers are known to have heterogeneous properties, and the NAC response may differ according to the tumor subtype [18]. According to Caudle et al. [5], the rate of PD differed between tumor subtypes, and patients with indolent hormone receptor-positive/human epidermal growth factor receptor 2-negative breast cancers rarely achieved pCR or experienced PD. In contrast, patients with highly proliferating TNBC achieved higher pCR rates and more often experienced PD [5]. Moreover, the survival outcomes of TNBC without achieving pCR are worse than those of other subtypes of breast cancer [19]. Therefore, we decided to focus on TNBC rather than pooling all subtypes.

This study investigated the association of clinical, pathologic, and MRI variables with PD during NAC and distant metastasis-free survival (DMFS) in patients with TNBC. Additionally, we aimed to develop models to predict these outcomes.

MATERIALS AND METHODS

This retrospective study was approved by the institutional review board of Seoul National University Hospital (IRB number: 2103-145-1206). The requirement for informed consent was waived.

Patients

Patients with TNBC at the time of the initial diagnosis who underwent NAC between January 2010 and December 2019 were identified in the Breast Cancer Registry of Seoul National University Hospital. The exclusion criteria were as follows: no available pre-NAC MRI images; received an off-protocol NAC regimen; recurrent breast cancer; presence of distant metastasis at the time of the initial diagnosis; bilateral breast cancer; and excisional biopsy performed before the initiation of NAC. Three previous studies included 27, 45, and 70 overlapping patients [20-22] and evaluated factors associated with the pCR. However, this study focused on predicting PD.

Clinical and Pathologic Data Collection and Patient Treatment

Patient age, clinical stage, surgery method, and adjuvant therapy data were collected by reviewing the electronic medical records. The histology type (ductal or metaplastic), nuclear grade (low, intermediate, or high), and Ki-67 index (%) were collected from the biopsy specimens before the initiation of NAC. Patients underwent either AC4-D4 (four cycles of doxorubicin [60 mg/m^2] plus cyclophosphamide [600 mg/m^2] followed by four cycles of docetaxel [75 mg/m^2]) or AD6 (six cycles of doxorubicin [50 mg/m^2] plus docetaxel [75 mg/m^2]) at the discretion of the oncology specialists. AC4-D4 was dominantly used after July 2013. The pathologic stage and lymphovascular invasion (LVI) of the surgical specimens were recorded.

MRI Acquisition and Image Analysis

We performed 1.5T MRI before September 2016; thereafter, we performed 3.0T MRI. The MRI protocols are shown in Supplementary Table 1. The pre-NAC MRI

 https://doi.org/10.3348/kjr.2022.0974

findings were independently reviewed according to the Breast Imaging Reporting and Data System lexicon by two dedicated breast radiologists (H.Y. and S.Y.K. with 3 years and 10 years of experience, respectively) [23]. Discordant results were re-evaluated to achieve a consensus. The radiologists were blinded to patient information, including tumor response and assessed tumor size, peritumoral edema, intratumoral necrosis, amount of fibroglandular tissue, background parenchymal enhancement, tumor type (mass or mass with non-mass enhancement), shape, margin, internal enhancement pattern, distribution of non-mass enhancement, and lesion multiplicity.

Peritumoral edema on fat-suppressed T2-weighted images was evaluated and classified as follows (Supplementary Fig. 1) [17,24]: no edema; peritumoral edema only; prepectoral edema with or without peritumoral edema; and subcutaneous edema with or without peritumoral or prepectoral edema. Intratumoral necrosis was defined as a nonenhancing area with high T2 signal intensity inside the mass [25,26].

Response Assessment

The patients were clinically examined by oncologists during each NAC cycle. Imaging was performed if PD was suspected. Imaging studies routinely performed during NAC included breast ultrasound before, during, and after NAC, breast MRI, and mammography before and after NAC.

We retrospectively evaluated the tumor response based on the RECIST criteria [27] by comparing the longest diameter measured on MRI before and after NAC. If post-NAC MRI images were unavailable, then we reviewed and compared ultrasound images before and after NAC (n = 6; 4 in the development set and 2 in the validation set). PD was considered when the longest diameter of the target lesion increased by more than 20% compared to the smallest measurement obtained during the previous examination and the absolute difference was more than 5 mm. Furthermore, if one or more new lesions appeared, then we considered that PD had developed.

Outcome Data Collection

To monitor distant metastasis, patients underwent follow-up evaluations including chest radiography and chest computed tomography every 6 months and bone scans and abdominal computed tomography or ultrasound every year at the physician's discretion. The DMFS was calculated as the time interval from the first use of NAC (time zero) to the discovery of distant metastasis (event). Patients who did not experience metastasis at the last follow-up visit were censored.

Statistical Analysis

Patients were randomly divided into the development and validation sets using a 2:1 ratio. In these two sets, the PD and non-PD groups were compared using the chi-squared test or independent *t*-test. In the development set, a multivariable logistic regression analysis with a stepwise method was performed to identify factors associated with PD, and a multivariable Cox regression analysis with backward elimination was performed to identify factors associated with DMFS. Variables with $P < 0.1$ in the univariable analyses were entered into the multivariable analyses. Kaplan-Meier curves for DMFS in the the development set were obtained. Prediction models for PD and DMFS were developed based on the multivariable analyses results [28]. The discrimination and calibration performances of the prediction models were tested using the validation set. Discrimination performance was evaluated using the area under the receiver-operating characteristic curve (AUC) for PD and Harrell's C-index for DMFS. The AUCs for PD of the two prediction models (clinical-pathologic and clinical-pathologic-MRI models) were compared [29]. We analyzed the time-dependent receiver-operating characteristic curve for 2-year DMFS. Interobserver agreement for MRI variables was evaluated using kappa for categorical variables and the intraclass correlation coefficient for continuous variables [30,31]. $P < 0.05$ was considered statistically significant. Statistical analyses were performed using SAS (version 9.4; SAS Institute) and STATA (version 15; StataCorp).

RESULTS

Patient Characteristics

We initially identified 460 patients with TNBC who underwent NAC between January 2010 and December 2019. Of these 460 patients, 208 were excluded because they were lacking pre-NAC MRI images (n = 87), received an off-protocol regimen (n = 58), had recurrent breast cancer (n = 22), had initial distant metastasis (n = 19), had bilateral cancer (n = 12), or underwent excisional biopsy (n = 10). After exclusion, a total of 252 patients (age, 48.3 ± 10.7 years) were included in this study (Fig. 1). Patients with clinical stage II or stage III TNBC underwent NAC with either AC4-D4 (78%; 197/252) or AD6 (22%;

https://doi.org/10.3348/kjr.2022.0974

Korean Journal of Radiology
KJR

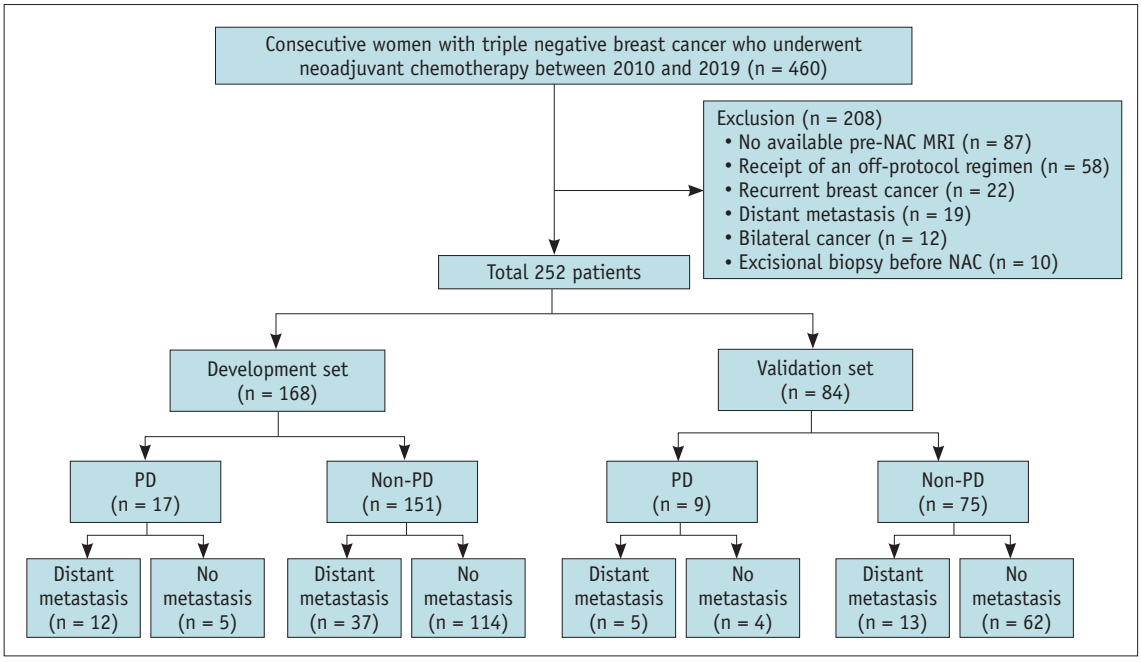

Fig. 1. Flowchart of patient selection and allocation to the development and validation sets. After exclusion, included 252 patients were randomly divided into the development and validation sets using a 2:1 ratio. NAC = neoadjuvant chemotherapy, PD = progressive disease, MRI = magnetic resonance imaging

55/252). Furthermore, they underwent breast-conserving surgery (65%; 163/252) or mastectomy (35%; 89/252) and adjuvant chemotherapy (32%; 80/252) or adjuvant radiation therapy (89%; 225/252) based on the consensus of the multidisciplinary discussion.

After surgical excision, pCR was achieved in 23% of patients (59/252); however, residual tumors in the breast or axillary lymph nodes were observed in 77% of patients (193/252). LVI was observed in 23% of patients (57/252). Among the 36 patients with subcutaneous edema on pre-NAC MRI images, LVI was confirmed after surgical resection in 15 patients (42%). Among patients without subcutaneous edema on pre-NAC MRI images, 19% had positive LVI (42/216).

Development and Validation Sets

Patients were randomly assigned to the development set (n = 168; age, 49.4 ± 10.8 years) or validation set (n = 84; age, 45.9 ± 10.4 years). All clinical, pathologic, and MRI characteristics were comparable between the two sets (Tables 1, 2) (all $P > 0.05$). In the development set, 17 of 168 patients (10%) had PD. In the validation set, 9 of 84 patients (11%) had PD. Among the 17 patients with PD in the development set, 12 had primary breast tumor progression, 4 had both breast and nodal lesions, and 1 developed lung metastasis. Of the nine patients with PD in the validation set, eight had primary breast tumor progression and one had progression of both the breast and nodal lesions. Distant metastases occurred in 49 of 168 patients (29%) in the development set and 18 of 84 patients (21%) in the validation set. The follow-up time did not differ between the two sets (52 ± 35 months vs. 55 ± 34 months; $P = 0.287$).

Treatment Response and Management of Patients with PD

Of the 26 patients considered to have PD, 22 were diagnosed with PD during NAC by oncologists. During imaging studies, all of these patients satisfied the RECIST criteria for PD. However, they did not complete the planned NAC regimen because of PD. Twenty patients underwent immediate surgery and two switched regimens and underwent surgery. Four of the 26 patients considered to have PD were eventually diagnosed with PD after the completion of NAC. Detailed information about the PD timeline and patient management is provided in Supplementary Table 2.

When the treatment methods and pathologic characteristics of the PD (n = 26) and non-PD (n = 226) groups were compared, it was found that the PD group underwent total mastectomy more frequently, and that axillary lymph node dissection and skin grafting were more often necessary. Patients in the PD group had a more advanced pathologic stage and were more likely to have LVI.

https://doi.org/10.3348/kjr.2022.0974

Table 1. Clinical and Pathologic Characteristics of the Development Set and Validation Set

Characteristics	Total (n = 252)	Development Set (n = 168)	Validation Set (n = 84)	*P*
Age (yr)	48.3 ± 10.7	49.4 ± 10.8	45.9 ± 10.4	0.836
AJCC clinical stage				0.208
Stage II	109 (43)	68 (40)	41 (49)	
Stage III	143 (57)	100 (60)	43 (51)	
Histologic type				> 0.999
Ductal	239 (95)	159 (95)	80 (95)	
Metaplastic	13 (5)	9 (5)	4 (5)	
Nuclear grade				0.426
Low or Intermediate	70 (28)	44 (26)	26 (31)	
High	182 (72)	124 (74)	58 (69)	
Ki-67 (%)	35 ± 25	35 ± 24	36 ± 27	0.723
NAC regimen				0.420
AD6	55 (22)	34 (20)	21 (25)	
AC4-D4	197 (78)	134 (80)	63 (75)	
Progressive disease	26 (10)	17 (10)	9 (11)	0.884
Breast surgery				0.926
Breast-conserving	163 (65)	109 (65)	54 (64)	
Mastectomy	89 (35)	59 (35)	30 (36)	
Axillary surgery				0.653
SLNB	143 (57)	97 (58)	46 (55)	
ALND	109 (43)	71 (42)	38 (45)	0.883
Pathologic stage				
pCR	59 (23)	38 (23)	21 (25)	
Invasive residual in the breast with no residual in lymph nodes	116 (46)	79 (47)	37 (44)	
Residual in both breast and lymph nodes	77 (31)	51 (30)	26 (31)	
Presence of lymphovascular invasion	57 (23)	36 (21)	21 (25)	0.523
Use of adjuvant chemotherapy	80 (32)	60 (36)	20 (24)	0.056
Use of adjuvant radiation therapy	225 (89)	149 (89)	76 (90)	0.666
Distant metastasis	67 (27)	49 (29)	18 (21)	0.190
Follow-up time (month)	44 ± 35	40 ± 35	47 ± 34	0.459

Values are presented as mean ± standard deviation or n (%) unless otherwise indicated. Pathologic complete response (pCR) was defined as no invasive residual in breast and lymph nodes (in situ breast residuals allowed). AJCC = American Joint Committee on Cancer, NAC = neoadjuvant chemotherapy, AD6 = six cycles of doxorubicin plus docetaxel, AC4-D4 = four cycles of doxorubicin plus cyclophosphamide followed by four cycles of docetaxel, SLNB = sentinel lymph node biopsy, ALND = axillary lymph node dissection

These patients also required adjuvant chemotherapy more often than the non-PD group. Adjuvant radiation therapy was performed less frequently in the PD group because breast-conserving surgery was performed less frequently (Supplementary Table 3) (all $P < 0.001$).

Factors Associated with PD in the Development Set

During the univariable analysis, the metaplastic histology ($P = 0.031$), Ki-67 index ($P = 0.046$), NAC regimen with AD6 ($P = 0.036$), and presence of subcutaneous edema ($P = 0.010$) on MRI images were associated with PD (Table 3). During the multivariable analysis that included only clinical and pathologic variables, only the metaplastic histology (odds ratio [OR], 5.0; 95% confidence interval [CI], 1.1–22.9; $P = 0.039$) was independently associated with PD. Ki-67 was associated with PD, but with marginal significance (OR, 1.02; 95% CI, 1.0–1.04; $P = 0.054$). During the multivariable analysis, which included clinical, pathologic, and MRI variables, the metaplastic histology (OR, 8.0; 95% CI, 1.2–53.8; $P = 0.032$), Ki-67 index (OR, 1.02; 95% CI, 1.001–1.05; $P = 0.044$), and subcutaneous edema (OR, 30.6; 95% CI, 2.0–153.9; $P = 0.004$) were independently associated with PD (Table 4).

https://doi.org/10.3348/kjr.2022.0974

Korean Journal of Radiology
KJR

Table 2. MRI Characteristics of the Development Set and Validation Set

Characteristics	Total (n = 252)	Development Set (n = 168)	Validation Set (n = 84)	*P*
Tumor size (cm)	4.3 ± 2.1	4.3 ± 2.0	4.2 ± 2.2	0.793
Edema degree				0.820
No edema	60 (24)	41 (24)	19 (23)	
Peritumoral edema only	100 (40)	62 (37)	38 (45)	
Prepectoral edema	56 (22)	42 (25)	14 (17)	
Subcutaneous edema	36 (14)	23 (14)	13 (15)	
Necrosis	157 (62)	104 (62)	53 (63)	0.854
FGT				0.593
Non-dense	32 (13)	20 (12)	12 (14)	
Dense	220 (87)	148 (88)	72 (86)	
BPE				0.841
Minimal/mild	184 (73)	122 (73)	62 (74)	
Moderate/marked	68 (27)	46 (27)	22 (26)	
Tumor type				0.252
Mass	171 (68)	110 (65)	61 (73)	
Mass with NME	81 (32)	58 (35)	23 (27)	
Mass shape				> 0.999
Round or Oval	18 (7)	12 (7)	6 (7)	
Irregular	234 (93)	156 (93)	78 (93)	
Mass margin				> 0.999
Circumscribed	4 (2)	3 (2)	1 (1)	
Irregular/spiculated	248 (98)	165 (98)	83 (99)	
Mass internal enhancement				0.163
Hetero	90 (36)	55 (33)	35 (42)	
Rim	162 (64)	113 (67)	49 (58)	
NME distribution*				0.329
Focal	4 (5)	4 (7)	0 (0)	
Linear/segmental	65 (80)	46 (79)	19 (83)	
Regional/diffuse	12 (15)	8 (14)	4 (17)	
NME internal enhancement*				0.364
Heterogeneous	52 (64)	39 (67)	13 (57)	
Clumped/clustered ring	29 (36)	19 (33)	10 (43)	
Multiplicity				0.079
Unifocal	177 (70)	112 (67)	65 (77)	
Multifocal or Multicentric	75 (30)	56 (33)	19 (23)	

Values are presented as mean ± standard deviation or n (%) unless otherwise indicated. *There were 81 lesions with associated NME in total patient, 58 lesions in the development set and 84 lesions in the validation set. The ratio was calculated accordingly. MRI = magnetic resonance imaging, FGT = fibroglandular tissue, BPE = background parenchymal enhancement, NME = non-mass enhancement

Prediction Model for PD

We developed a prediction model for PD based on the clinical, pathologic, and MRI variables as follows:

$$\text{Risk (probability of PD)} = \frac{1}{1+e^{-Z}}$$

where Z = 1.2026 * Edema1 + 2.1031 * Edema2 + 3.4221 * Edema3 + 2.0846 * Histology type + 0.0230 * Ki-67 - 5.1280. Edema1 indicated peritumoral edema only, Edema2 indicated prepectoral edema (with or without peritumoral edema), and Edema3 indicated subcutaneous edema (with or without peritumoral and prepectoral edema). The histologic type was coded as 0 (ductal type) or 1 (metaplastic type). The Ki-67 index was included in the equation as a continuous variable.

In the development set, the clinical-pathologic-MRI

 https://doi.org/10.3348/kjr.2022.0974

Table 3. Univariable Analysis for Predictors of Progression of Disease (PD) in the Development Set (n = 168)

	Non-PD (n = 151)	PD (n = 17)	Odds Ratio	95% CI	*P*
Clinical and pathologic					
Age (yr)	48.2 ± 10.6	46.1 ± 9.2	0.99	0.9–1.04	0.422
AJCC clinical stage					
Stage II	64 (42)	4 (24)	Reference		
Stage III	87 (58)	13 (76)	2.4	0.7–7.7	0.143
Histologic type					
Ductal	145 (96)	14 (82)	Reference		
Metaplastic	6 (4)	3 (18)	5.2	1.2–23.0	0.031
Nuclear grade					
Low or Intermediate	42 (28)	2 (12)	Reference		
High	109 (72)	15 (88)	2.9	0.6–13.2	0.171
Ki-67 (%)	34 ± 23	46 ± 28	1.02	1.00–1.04	0.046
NAC regimen					
AC4-D4	124 (82)	10 (59)	Reference		
AD6	27 (18)	7 (41)	3.2	1.1–9.2	0.036
MRI					
Tumor size (cm)	4.2 ± 2.0	5.2 ± 2.1	1.24	0.99–1.6	0.060
Edema degree					0.007
No edema	40 (26)	1 (6)	Reference		
Peritumoral edema only	59 (39)	3 (18)	2	0.2–20.3	0.545
Prepectoral edema	36 (24)	6 (35)	6.7	0.8–58.1	0.086
Subcutaneous edema	16 (11)	7 (41)	17.5	2.0–153.9	0.010
Necrosis	92 (61)	12 (71)	1.5	0.5–4.6	0.440
FGT					
Non-dense	19 (13)	1 (6)	Reference		
Dense	132 (87)	16 (94)	2.3	0.3–18.4	0.431
BPE					
Minimal/mild	112 (74)	10 (59)	Reference		
Moderate/marked	39 (26)	7 (41)	2.0	0.7–5.6	0.185
Tumor type					
Mass	100 (66)	10 (59)	Reference		
Mass with NME	51 (34)	7 (41)	1.4	0.5–3.8	0.544
Mass shape					
Round or Oval	12 (8)	0 (0)	Reference		
Irregular	139 (92)	17 (100)	3.1	0.4–408.3	0.453
Mass margin					
Circumscribed	3 (2)	0 (0)	Reference		
Irregular/spiculated	148 (98)	17 (100)	0.8	0.1–112.7	0.913
Mass internal enhancement					
Hetero	52 (34)	3 (18)	Reference		
Rim	99 (66)	14 (82)	2.5	0.7–8.9	0.174
NME distribution*					0.489
Focal	4 (8)	0 (0)	Reference		
Linear/segmental	41 (80)	5 (71)	1.2	0.1–166.1	0.918
Regional/diffuse	6 (12)	2 (29)	3.5	0.2–523.6	0.501
NME internal enhancement*					
Heterogeneous	34 (67)	5 (71)	Reference		
Clumped/clustered ring	17 (33)	2 (29)	0.8	0.1–4.6	0.802
Multiplicity					
Unifocal	101 (67)	11 (65)	Reference		
Multifocal or Multicentric	50 (33)	6 (35)	1.1	0.4–3.2	0.857

Values are presented as mean ± standard deviation or n (%) unless otherwise indicated. *There were 81 lesions with associated NME in total patient, 58 lesions in the development set and 84 lesions in the validation set. The ratio was calculated accordingly. CI = confidence interval, AJCC = American Joint Committee on Cancer, NAC = neoadjuvant chemotherapy, AC4-D4 = four cycles of doxorubicin plus cyclophosphamide followed by four cycles of docetaxel, AD6 = six cycles of doxorubicin plus docetaxel, MRI = magnetic resonance imaging, FGT = fibroglandular tissue, BPE = background parenchymal enhancement, NME = non-mass enhancement

https://doi.org/10.3348/kjr.2022.0974

Korean Journal of Radiology
KJR

model (which included with clinical, pathologic, and MRI variables) had significantly better discrimination ability to predict PD than the clinical-pathologic model (AUC, 0.86 [95% CI, 0.79–0.93] vs. 0.68 [95% CI, 0.53–0.83]; *P* = 0.025). In the validation set, the clinical-pathologic-MRI model also had significantly better discrimination ability to predict PD than the clinical-pathologic model (AUC, 0.69 [95% CI, 0.50–0.88] vs. 0.54 [95% CI, 0.35–0.73]; *P* = 0.017) (Fig. 2A). The prediction model was appropriately calibrated (Fig. 2B).

Table 4. Multivariable Analysis for Predictors of Progression of Disease in the Development Set (n = 168)

	Odds Ratio	95% CI	*P*
Clinical-pathologic model			
Histology type			
Ductal	Reference		
Metaplastic	5.0	1.1–22.9	0.039
Ki-67 (%)	1.02	1.0–1.04	0.054
Clinical-pathologic-MRI model			
Histology type			
Ductal	Reference		
Metaplastic	8.0	1.2–53.8	0.032
Ki-67 (%)	1.02	1.001–1.05	0.044
Edema degree			0.005
No edema	Reference		
Peritumoral edema only	3.3	0.3–37.2	0.329
Prepectoral edema	8.2	0.8–58.1	0.068
Subcutaneous edema	30.6	2.0–153.9	0.004

CI = confidence interval, MRI = magnetic resonance imaging

Factors Associated with DMFS in the Development Set

During the univariable analysis, clinical stage III (*P* < 0.001), NAC regimen with AD6 (*P* = 0.008), PD (*P* < 0.001), total mastectomy (*P* < 0.001), axillary lymph node dissection (*P* < 0.001), adjuvant chemotherapy (*P* = 0.005), no adjuvant radiotherapy (*P* = 0.012), residual disease in both the breast and lymph nodes (*P* < 0.001), presence of LVI (*P* < 0.001), large tumor size (*P* = 0.004), and presence of subcutaneous edema on MRI (*P* = 0.031) were associated with worse DMFS (Supplementary Table 4).

During the multivariable analysis, residual disease in both the breast and lymph nodes (hazard ratio [HR], 6.0; 95% CI, 1.7–21.2; *P* = 0.005) and the presence of LVI (HR, 3.3; 95% CI, 1.7–6.1; *P* < 0.001) were independently associated with DMFS (Table 5). Kaplan-Meier curves demonstrated significantly different DMFS according to the pathologic stage (Supplementary Fig. 2A) and LVI (Supplementary Fig. 2B).

Prediction Model for DMFS

A prediction model for DMFS, including the specific

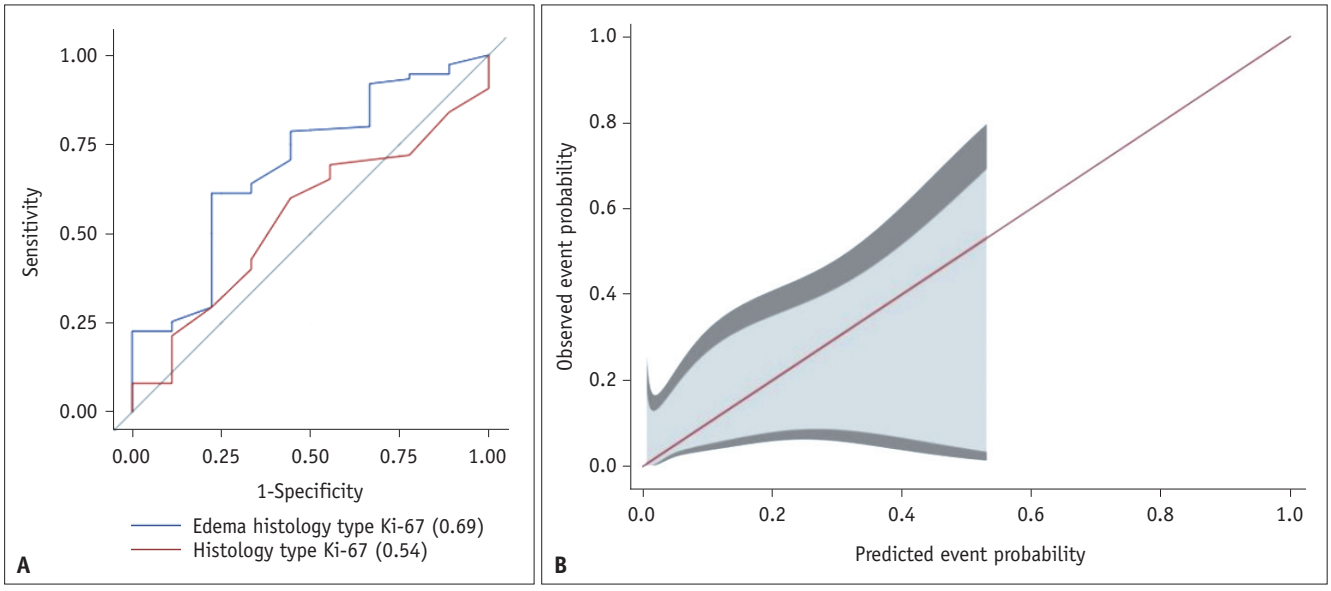

Fig. 2. Performance of the clinical-pathologic model (red line) and clinical-pathologic-magnetic resonance imaging (MRI) model (blue line) for predicting progressive disease in the validation set. **A:** Receiver-operating characteristic curves show the discrimination performance. Numbers in parentheses are areas under the receiver-operting characteristic curve. Adding information about subcutaneous edema to the clinical-pathologic model improved the diagnostic performance (0.69 vs. 0.54; *P* = 0.017). **B:** In this calibration plot for the clinical-pathologic-MRI model, the diagonal line indicates a reference line, the light gray area represents the 95% confidential interval (CI), and the dark gray area indicates the 99% CI. The reference line was included in the range of the 99% CI and *P* = 0.1, indicating that this plot was adequately calibrated.

https://doi.org/10.3348/kjr.2022.0974

Table 5. Multivariable Analysis for Predictors of Distant Metastasis-free Survival in the Development Set (n = 168)

	Hazard Ratio	95% CI	*P*
Pathologic stage			0.001
pCR	Reference		
Invasive residual in the breast with no residual in lymph nodes	2.1	0.6–7.3	0.248
Residual in both breast and lymph nodes	6.0	1.7–21.2	0.005
Lymphovascular invasion			
No	Reference		
Yes	3.3	1.7–6.1	< 0.001

Pathologic complete response (pCR) was defined as no invasive residual in the breast and lymph nodes (in situ breast residuals allowed).
CI = confidence interval

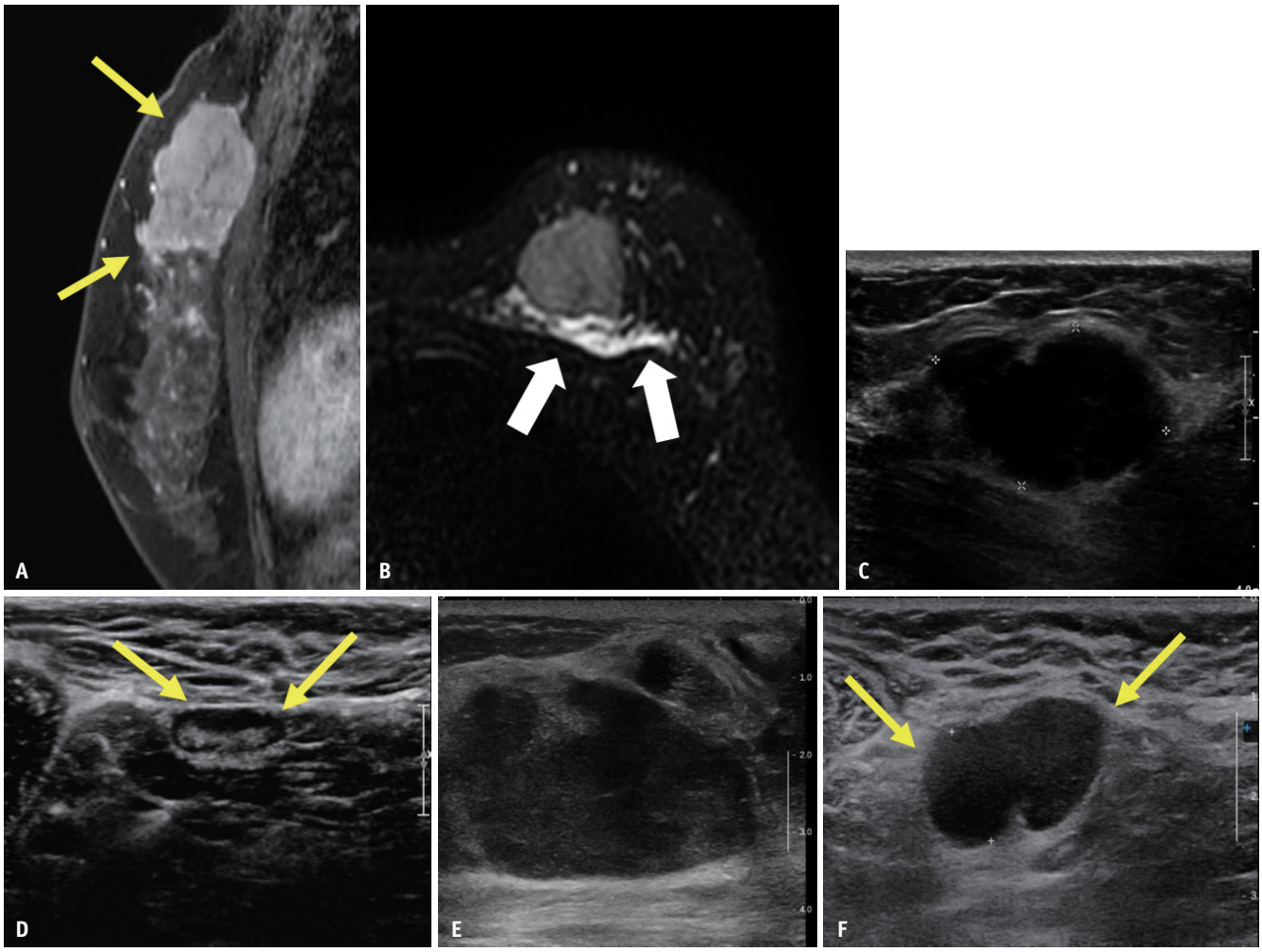

Fig. 3. Representative images of a 45-year-old woman with triple-negative breast cancer. **A:** Sagittal contrast-enhanced T1-weighted magnetic resonance imaging (MRI) image shows an irregular heterogeneously enhancing mass in the left upper breast (arrows). **B:** Axial fat-suppressed T2-weighted MRI shows prepectoral edema (arrows). After the ultrasound (US)-guided biopsy, the tumor showed metaplastic histology and the Ki-67 index was 80%. The calculated probability of progressive disease (PD) was 71%. **C, D:** Initial US images show a 3.7-cm irregular hypoechoic mass with only oval reactive lymph nodes in the ipsilateral axilla (arrows). **E, F:** After one cycle of chemotherapy with adriamycin and cyclophosphamide (AC1), the mass increased to 8.4 cm, and the ipsilateral axillary lymph node also increased (arrows). Consequently, it was determined to be PD. She underwent total mastectomy, and the surgical histopathologic examination showed a residual of 9.1 cm with extensive lymphatic and vascular emboli. Of the 30 resected axillary lymph nodes, there were 18 metastatic lymph nodes. Thus, the calculated probability of distant metastasis within 2 years was 19.3%. Bone metastasis was observed 6 months postoperatively.

https://doi.org/10.3348/kjr.2022.0974

Korean Journal of Radiology
KJR

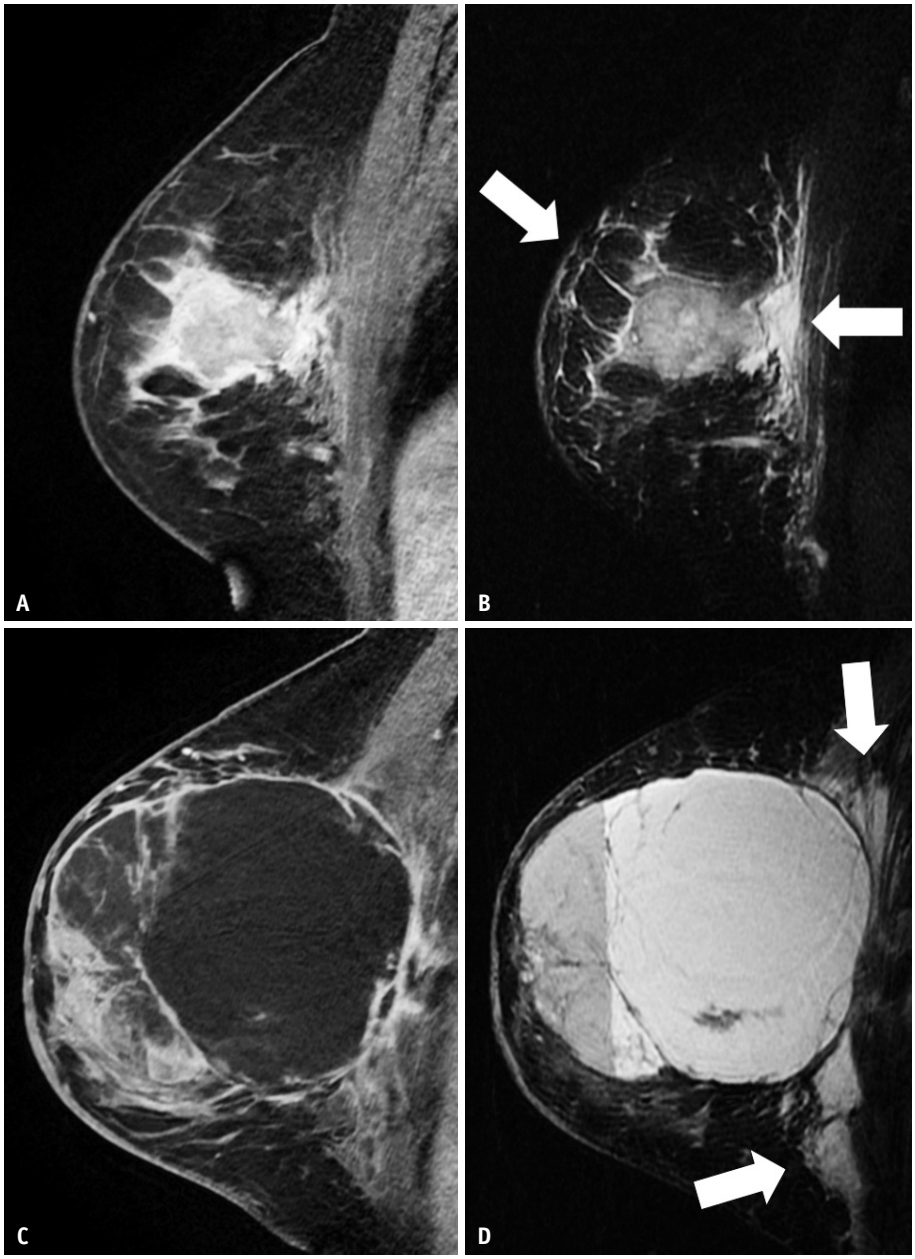

Fig. 4. Representative magnetic resonance imaging (MRI) images of a 53-year-old woman with triple-negative breast cancer in her right breast. **A:** Sagittal contrast-enhanced T1-weighted MRI image shows an irregular heterogeneously enhancing 4.5-cm mass in the right breast. **B:** On sagittal fat-suppressed T2-weighted MRI, extensive peritumoral edema was observed in the subcutaneous and prepectoral areas (arrows). A core needle biopsy confirmed the ductal histology type, and the Ki-67 index was 80%. Therefore, the calculated progressive disease probability was 53.3%. **C:** After the first cycle of neoadjuvant chemotherapy with adriamycin and cyclophosphamide, the size of the primary lesion increased to 11.4 cm. **D:** Intratumoral necrosis and prepectoral edema (arrows) in the tumor are aggravated. Although taxane was administered, there was no response. Consequently, the patient underwent total mastectomy. Histopathology results showed no lymphovascular invasion, and the tumor was diagnosed as 5.5-cm residual invasive cancer of the breast. The calculated probability of distant metastasis was 2.1%, and no distant metastasis was observed during 88.6 months of follow-up.

prediction of 2-year DMFS, was developed using pathologic variables based on the multivariable Cox regression analysis as follows:

$$\text{Probability of DMFS} = C * e^{0.73616 * \text{Stage1} + 1.79657 * \text{Stage2} + 1.17872 * \text{LVI}}$$

C was set as 0.98522 for 2-year DMFS.

Variables were coded as 0 (no) or 1 (yes) for LVI. The stages were coded as stage 1 (invasive residual disease in the breast with no residual disease in the lymph nodes) or stage 2 (residual disease in both the breast and lymph

 https://doi.org/10.3348/kjr.2022.0974

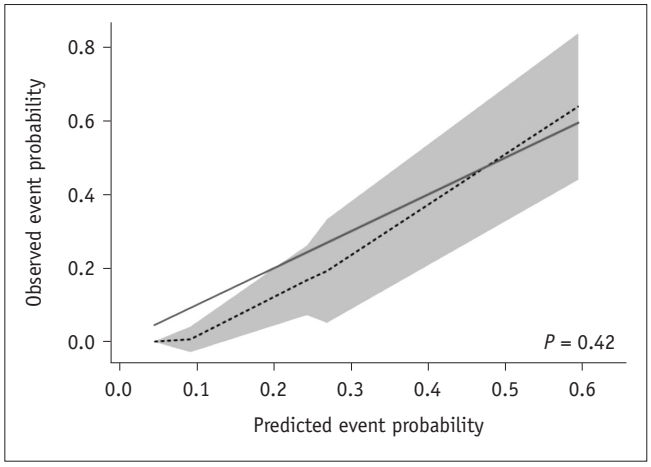

Fig. 5. Calibration plot of 2-year distant metastasis-free survival of the validation set. The diagonal solid line indicates the reference line, and the dashed line is the calibration curve. The gray area represents the 95% confidence intervals. The intercept and slope of the dashed calibration curve were not significantly different compared to those of the reference line, suggesting good calibration (P = 0.42).

nodes). The representative PD cases with and without distant metastasis are presented in Figure 3 and 4, respectively.

The prediction model showed good discrimination ability in the development set (Harrell's C-index, 0.76; 95% CI, 0.70–0.83) and validation set (Harrell's C-index, 0.86; 95% CI, 0.80–0.92). A time-dependent receiver-operating characteristic curve was estimated for the 2-year follow-up time, and the AUC was 0.91 (95% CI, 0.84-0.99) in the validation set. The prediction model was well-calibrated for 2-year DMFS in the validation set (Fig. 5).

Interobserver Agreement for MRI Variables

Interobserver agreement for the MRI variables was heterogeneous, ranging from fair to almost perfect (Supplementary Table 5). The agreement for edema was substantial (kappa = 0.64).

DISCUSSION

Little is known about the predictors of PD. We found that the metaplastic histology (OR, 8.0; P = 0.032) and Ki-67 index (OR 1.02, P = 0.044) obtained from pre-NAC biopsy specimens and subcutaneous edema (OR, 30.6; P = 0.004) identified on pre-NAC MRI images were independently associated with PD in the development set (n = 168). The clinical-pathologic-MRI model including MRI edema performed better than the clinical-pathologic model. However, the performance of the clinical-pathologic-MRI model decreased to 0.69 in the validation set (n = 84). This decrease in performance may have been attributable to the insufficient sample size of the validation set or model overfitting in the development set. In terms of survival outcomes, the presence of residual disease in both the breast and lymph nodes (HR, 6.0; P = 0.005) and LVI (HR, 3.3; P < 0.001) were independently associated with worse DMFS.

Among various pre-NAC MRI factors, only subcutaneous edema was independently associated with PD. During the final stage of breast edema, subcutaneous edema is associated with extensive LVI in the breast and is thought to be caused by the blockage of lymphatic drainage in dermal and subdermal areas [24]. Although edema was evaluated using pre-NAC MRI rather than post-NAC MRI and the pathologic report reflected the status of the tumor bed after chemotherapy completion, LVI remained in 15 of 36 patients who presented with subcutaneous edema at the time of pre-NAC MRI (42%). In contrast, only 19% (42/216) of patients without subcutaneous edema had LVI during the pathologic examination. Extensive LVI is also associated with chemoresistance [32]. Thus, the higher risk of PD with the presence of subcutaneous edema on MRI is thought to be mediated by LVI. Therefore, for patients with subcutaneous edema on pre-NAC MRI images, the NAC response should be closely monitored and an early switch to surgical resection should be considered.

Among the clinical and pathologic factors, the metaplastic histology and Ki-67 index were independently associated with PD. This was consistent with previous studies that showed that the metaplastic type is less sensitive to chemotherapy and has a poorer prognosis than the ductal type [33,34]. However, metaplastic histology is a limited predictor because of its infrequent incidence (< 5% of total TNBC cases) and the limited accuracy of core needle biopsy specimens [33]. As a proliferation marker, a high Ki-67 index is associated with a pCR [35]; therefore, it is not a specific marker for predicting PD. Moreover, the representativeness of core needle biopsy specimens and the appropriate cutoff for dividing high and low levels of the Ki-67 index are controversial [36]. The clinical-pathologic model consisting of the metaplastic histology and Ki-67 index showed suboptimal performance for predicting PD.

Regarding survival outcomes, unlike the study by Caudle et al. [5], PD was not independently associated with worse DMFS after the multivariable analysis in our study. This discrepancy may be explained by differences in the tumor

https://doi.org/10.3348/kjr.2022.0974

Korean Journal of Radiology
KJR

subtype, race, PD determination method, and variables included in the multivariable analysis. Our study evaluated TNBC in Asian women and determined the PD status using imaging examination results and RECIST criteria. In contrast, Caudle et al. [5] evaluated all tumor subtypes (total = 1928; TNBC = 167) of women of various races, and the imaging examination results and RECIST criteria were not mandatory for determining PD. However, during our study, the pathologic stage, rather than PD itself, after the multivariable analysis was more strongly associated with DMFS.

According to our study, if PD is promptly identified by proper monitoring during NAC, and if patients with PD undergo proper management, such as switching chemotherapy regimens or immediate surgery, then PD itself does not affect survival outcomes. The high residual tumor burden and LVI of the surgical specimen were independently associated with worse DMFS, consistent with the results of previous studies [19,37]. Furthermore, the prediction model combining the residual tumor burden and LVI showed acceptable discrimination performance for predicting DMFS in the development and validation sets. Therefore, the residual tumor burden and LVI should be considered during the risk assessment and postoperative management of patients with TNBC.

Our study had some limitations. First, patient selection bias may have been inevitable because this was a retrospective study conducted at a single academic institution. We excluded 150 of the initial 402 patients. One of the main reasons for exclusion was the lack of available pre-NAC MRI images (n = 87). Second, the sample size was limited because PD is rare; however, we collected 10 years of data. Third, we did not perform external validation, which is necessary to confirm the reliability and generalizability of the prediction models. Fourth, heterogeneous interobserver agreement was observed between the two radiologists when evaluating qualitative MRI features. Fifth, we included patients who underwent two types of chemotherapy regimens and were evaluated using two types of MRI. Most patients with PD undergo immediate surgery rather than switching chemotherapy regimens. The differences in radiologists, treatment patterns, and MRI settings may have affected the results.

In conclusion, the clinical-pathologic-MRI model, which considers subcutaneous edema on MRI in addition to clinical and pathologic features, had better ability to predict PD with TNBC. However, MRI did not independently contribute to the prediction of DMFS.

Supplement

The Supplement is available with this article at https://doi.org/10.3348/kjr.2022.0974.

Availability of Data and Material

The datasets generated or analyzed during the study are available from the corresponding author on reasonable request.

Conflicts of Interest

Han-Byoel Lee is a co-founder and a member of the board of directors at DCGen Co., Ltd. Han-Byoel Lee received research funding from Devicor Medical Product, Inc., and consulting fees and honoraria from Alvogen, Boryung, Lilly, Novartis, Roche, Takeda, and Celltrion Pharm, outside of the current study. Other authors have no potential conflicts of interest to disclose.

Author Contributions

Conceptualization: Soo-Yeon Kim. Data curation: Heera Yoen, Soo-Yeon Kim. Formal analysis: Heera Yoen, Soo-Yeon Kim. Investigation: Heera Yoen, Soo-Yeon Kim, Dae-Won Lee, Han-Byoel Lee. Methodology: Soo-Yeon Kim. Project administration: Soo-Yeon Kim. Resources: Soo-Yeon Kim. Supervision: Soo-Yeon Kim. Writing—original draft: Heera Yoen, Soo-Yeon Kim. Writing—review & editing: all authors.

ORCID iDs

Heera Yoen
https://orcid.org/0000-0001-5583-6065
Soo-Yeon Kim
https://orcid.org/0000-0001-8915-3924
Dae-Won Lee
https://orcid.org/0000-0001-7133-6669
Han-Byoel Lee
https://orcid.org/0000-0003-0152-575X
Nariya Cho
https://orcid.org/0000-0003-4290-2777

Funding Statement

None

Acknowledgments

The statistical analyses were supported by the Medical Research Collaborating Center (MRCC) of Seoul National University. We sincerely thank Professor Yunhee Choi of

MRCC for her statistical assistance and consultation.

REFERENCES

1. Newman LA, Reis-Filho JS, Morrow M, Carey LA, King TA. The 2014 Society of Surgical Oncology Susan G. Komen for the Cure Symposium: triple-negative breast cancer. *Ann Surg Oncol* 2015;22:874-882
2. Foulkes WD, Smith IE, Reis-Filho JS. Triple-negative breast cancer. *N Engl J Med* 2010;363:1938-1948
3. Korde LA, Somerfield MR, Carey LA, Crews JR, Denduluri N, Hwang ES, et al. Neoadjuvant chemotherapy, endocrine therapy, and targeted therapy for breast cancer: ASCO guideline. *J Clin Oncol* 2021;39:1485-1505
4. Caudle AS, Gonzalez-Angulo AM, Hunt KK, Pusztai L, Kuerer HM, Mittendorf EA, et al. Impact of progression during neoadjuvant chemotherapy on surgical management of breast cancer. *Annals of Surgical Oncology* 2011;18:932-938
5. Caudle AS, Gonzalez-Angulo AM, Hunt KK, Liu P, Pusztai L, Symmans WF, et al. Predictors of tumor progression during neoadjuvant chemotherapy in breast cancer. *J Clin Oncol* 2010;28:1821-1828
6. Rouzier R, Pusztai L, Delaloge S, Gonzalez-Angulo AM, Andre F, Hess KR, et al. Nomograms to predict pathologic complete response and metastasis-free survival after preoperative chemotherapy for breast cancer. *J Clin Oncol* 2005;23:8331-8339
7. Keam B, Im SA, Park S, Nam BH, Han SW, Oh DY, et al. Nomogram predicting clinical outcomes in breast cancer patients treated with neoadjuvant chemotherapy. *J Cancer Res Clin Oncol* 2011;137:1301-1308
8. Colleoni M, Bagnardi V, Rotmensz N, Viale G, Mastropasqua M, Veronesi P, et al. A nomogram based on the expression of Ki-67, steroid hormone receptors status and number of chemotherapy courses to predict pathological complete remission after preoperative chemotherapy for breast cancer. *Eur J Cancer* 2010;46:2216-2224
9. Xu W, Chen X, Deng F, Zhang J, Zhang W, Tang J. Predictors of neoadjuvant chemotherapy response in breast cancer: a review. *Onco Targets Ther* 2020;13:5887-5899
10. Reig B, Heacock L, Lewin A, Cho N, Moy L. Role of MRI to assess response to neoadjuvant therapy for breast cancer. *J Magn Reson Imaging* 2020;52:1587-1606
11. Marinovich ML, Houssami N, Macaskill P, Sardanelli F, Irwig L, Mamounas EP, et al. Meta-analysis of magnetic resonance imaging in detecting residual breast cancer after neoadjuvant therapy. *J Natl Cancer Inst* 2013;105:321-333
12. Bian T, Wu Z, Lin Q, Wang H, Ge Y, Duan S, et al. Radiomic signatures derived from multiparametric MRI for the pretreatment prediction of response to neoadjuvant chemotherapy in breast cancer. *Br J Radiol* 2020;93:20200287
13. Sutton EJ, Onishi N, Fehr DA, Dashevsky BZ, Sadinski M, Pinker K, et al. A machine learning model that classifies breast cancer pathologic complete response on MRI post-neoadjuvant chemotherapy. *Breast Cancer Res* 2020;22:57
14. Goorts B, Dreuning KMA, Houwers JB, Kooreman LFS, Boerma EG, Mann RM, et al. MRI-based response patterns during neoadjuvant chemotherapy can predict pathological (complete) response in patients with breast cancer. *Breast Cancer Res* 2018;20:34
15. Gu YL, Pan SM, Ren J, Yang ZX, Jiang GQ. Role of magnetic resonance imaging in detection of pathologic complete remission in breast cancer patients treated with neoadjuvant chemotherapy: a meta-analysis. *Clin Breast Cancer* 2017;17:245-255
16. Yuan Y, Chen XS, Liu SY, Shen KW. Accuracy of MRI in prediction of pathologic complete remission in breast cancer after preoperative therapy: a meta-analysis. *AJR Am J Roentgenol* 2010;195:260-268
17. Harada TL, Uematsu T, Nakashima K, Kawabata T, Nishimura S, Takahashi K, et al. Evaluation of breast edema findings at T2-weighted breast MRI is useful for diagnosing occult inflammatory breast cancer and can predict prognosis after neoadjuvant chemotherapy. *Radiology* 2021;299:53-62
18. Gradishar WJ, Anderson BO, Abraham J, Aft R, Agnese D, Allison KH, et al. Breast cancer, version 3.2020, NCCN clinical practice guidelines in oncology. *J Natl Compr Canc Netw* 2020;18:452-478
19. Liedtke C, Mazouni C, Hess KR, André F, Tordai A, Mejia JA, et al. Response to neoadjuvant therapy and long-term survival in patients with triple-negative breast cancer. *J Clin Oncol* 2008;26:1275-1281
20. Bae MS, Shin SU, Ryu HS, Han W, Im SA, Park IA, et al. Pretreatment MR imaging features of triple-negative breast cancer: association with response to neoadjuvant chemotherapy and recurrence-free survival. *Radiology* 2016;281:392-400
21. Kim SY, Cho N, Park IA, Kwon BR, Shin SU, Kim SY, et al. Dynamic contrast-enhanced breast MRI for evaluating residual tumor size after neoadjuvant chemotherapy. *Radiology* 2018;289:327-334
22. Kim SY, Cho N, Choi Y, Lee SH, Ha SM, Kim ES, et al. Factors affecting pathologic complete response following neoadjuvant chemotherapy in breast cancer: development and validation of a predictive nomogram. *Radiology* 2021;299:290-300
23. American College of Radiology. *ACR BI-RADS Atlas: breast imaging reporting and data system; mammography, ultrasound, magnetic resonance imaging, follow-up and outcome monitoring, data dictionary,* 5th ed. Reston: American College of Radiology, 2013:1-173
24. Uematsu T. Focal breast edema associated with malignancy on T2-weighted images of breast MRI: peritumoral edema, prepectoral edema, and subcutaneous edema. *Breast Cancer* 2015;22:66-70
25. Kim SY, Kim EK, Moon HJ, Yoon JH, Koo JS, Kim SG, et al. Association among T2 signal intensity, necrosis, ADC and Ki-67 in estrogen receptor-positive and HER2-negative invasive ductal carcinoma. *Magn Reson Imaging* 2018;54:176-182

https://doi.org/10.3348/kjr.2022.0974

26. Harada TL, Uematsu T, Nakashima K, Sugino T, Nishimura S, Takahashi K, et al. Is the presence of edema and necrosis on T2WI pretreatment breast MRI the key to predict pCR of triple negative breast cancer? *Eur Radiol* 2020;30:3363-3370
27. Eisenhauer EA, Therasse P, Bogaerts J, Schwartz LH, Sargent D, Ford R, et al. New response evaluation criteria in solid tumours: revised RECIST guideline (version 1.1). *Eur J Cancer* 2009;45:228-247
28. Harrell FE Jr, Lee KL, Mark DB. Multivariable prognostic models: issues in developing models, evaluating assumptions and adequacy, and measuring and reducing errors. *Stat Med* 1996;15:361-387
29. DeLong ER, DeLong DM, Clarke-Pearson DL. Comparing the areas under two or more correlated receiver operating characteristic curves: a nonparametric approach. *Biometrics* 1988:837-845
30. Landis JR, Koch GG. The measurement of observer agreement for categorical data. *Biometrics* 1977:159-174
31. Koo TK, Li MY. A guideline of selecting and reporting intraclass correlation coefficients for reliability research. *J Chiropr Med* 2016;15:155-163
32. Uematsu T, Kasami M, Watanabe J, Takahashi K, Yamasaki S, Tanaka K, et al. Is lymphovascular invasion degree one of the important factors to predict neoadjuvant chemotherapy efficacy in breast cancer? *Breast Cancer* 2011;18:309-313
33. González-Martínez S, Pérez-Mies B, Carretero-Barrio I, Palacios-Berraquero ML, Perez-García J, Cortés J, et al. Molecular features of metaplastic breast carcinoma: an infrequent subtype of triple negative breast carcinoma. *Cancers (Basel)* 2020;12:1832
34. Park HS, Park S, Kim JH, Lee JH, Choi SY, Park BW et al. Clinicopathologic features and outcomes of metaplastic breast carcinoma: comparison with invasive ductal carcinoma of the breast. *Yonsei Med J* 2010;51:864-869
35. Chen X, He C, Han D, Zhou M, Wang Q, Tian J, et al. The predictive value of Ki-67 before neoadjuvant chemotherapy for breast cancer: a systematic review and meta-analysis. *Future Oncol* 2017;13:843-857
36. Holanek M, Selingerova I, Fabian P, Coufal O, Zapletal O, Petrakova K, et al. Biomarker dynamics and long-term treatment outcomes in breast cancer patients with residual cancer burden after neoadjuvant therapy. *Diagnostics (Basel)* 2022;12:1740
37. Hamy AS, Lam GT, Laas E, Darrigues L, Balezeau T, Guerin J, et al. Lymphovascular invasion after neoadjuvant chemotherapy is strongly associated with poor prognosis in breast carcinoma. *Breast Cancer Res Treat* 2018;169:295-304